
This is an electronic reprint of the original article.
This reprint may differ from the original in pagination and typographic detail.

Jeon, Junmo; Kwon, Sun-Yong; Lindberg, Daniel; Paek, Min

Thermodynamic Modeling of Ni-C, Co-C, and Ni-Co-C Liquid Alloys Using the Modified Quasichemical Model

Published in:

Metallurgical and Materials Transactions B: Process Metallurgy and Materials Processing Science

DOI:

[10.1007/s11663-020-01995-6](https://doi.org/10.1007/s11663-020-01995-6)

Published: 01/02/2021

Document Version

Publisher's PDF, also known as Version of record

Published under the following license:

CC BY

Please cite the original version:

Jeon, J., Kwon, S.-Y., Lindberg, D., & Paek, M. (2021). Thermodynamic Modeling of Ni-C, Co-C, and Ni-Co-C Liquid Alloys Using the Modified Quasichemical Model. *Metallurgical and Materials Transactions B: Process Metallurgy and Materials Processing Science*, 52(1), 59-68. <https://doi.org/10.1007/s11663-020-01995-6>

This material is protected by copyright and other intellectual property rights, and duplication or sale of all or part of any of the repository collections is not permitted, except that material may be duplicated by you for your research use or educational purposes in electronic or print form. You must obtain permission for any other use. Electronic or print copies may not be offered, whether for sale or otherwise to anyone who is not an authorised user.

Thermodynamic Modeling of Ni-C, Co-C, and Ni-Co-C Liquid Alloys Using the Modified Quasichemical Model



JUNMO JEON, SUN-YONG KWON, DANIEL LINDBERG, and MIN-KYU PAEK

The strong interactions between the metallic elements and C in liquid Ni, Co, and Ni-Co alloys have been thermodynamically analyzed. The liquid solution properties in Ni-C and Co-C systems showed significant asymmetry because of the short-range ordering of C exhibited in the liquid solution. Using the modified quasichemical model in the pair approximation, the Ni-C and Co-C systems were re-optimized to simultaneously reproduce the present experimental results of the C solubility and the reported thermodynamic properties in the liquid phases. In particular, the partial enthalpy data of C in liquid Ni and Co alloys were considered for the first time on the thermodynamic assessment of Ni-C and Co-C liquid solutions. The asymmetric interpolation method was introduced to evaluate the Gibbs free energy in the ternary system based on the binary Gibbs free energies in the Ni-C and Co-C systems. The C solubility data measured in the ternary Ni-Co-C alloy melt over a wide Co concentration range were successfully reproduced without any additional ternary model parameter by considering the short-range ordering of C.

<https://doi.org/10.1007/s11663-020-01995-6>
© The Author(s) 2020

I. INTRODUCTION

NICKEL and cobalt are critical raw materials for high-tech products and emerging industries. They have been utilized for lithium-ion batteries and nickel metal-hydride batteries as well as aerospace structural materials, so-called superalloys.^[1-5] For lithium-ion batteries, they contribute to promoting the stable structure and high capacity of cathode materials.^[1] The Ni-Co rechargeable battery has been suggested as a potential power source of nickel metal-hydride batteries because of the high energy capacity and long durability.^[2] The addition of Co has enhanced the creep rupture lives of Ni-based superalloys.^[5] With such increasing

demand for Ni and Co, their prices have increased, and the supply challenges of the alloys also have risen.^[6] Therefore, the recycling of these valuable metals from industrial secondary resources has become an essential substitute for securing critical resources.

There have been several attempts to recycle Ni and Co from industrial battery scrap in the Ni slag cleaning process to overcome the conventional hydrometallurgical process, which causes various unattractive byproducts such as toxic gases, acidic wastewater, salt, and organic solvent.^[7-9] The discarded batteries and Ni-Co alloy scraps are excellent resources along with dried Ni concentrate for the Ni flash smelting furnace. In the pyrometallurgical extraction process, the carbon can be easily dissolved in the liquid Ni and Co alloy as it is derived from the battery scrap or reducing agents such as cokes and coal. Since C can be dissolved up to 2 to 3 mass pct in the liquid Ni-Co alloy during the high-temperature carbothermic reaction, it influences the recycling efficiency as well as the properties of the final products. To find the optimum condition of the recycling process, it is required to know the basic information such as the distribution behavior of alloying elements and impurities and heat loss by adding the waste materials, and so on. These can be only predicted by accurate thermodynamic data of the activity, an activity coefficient of each element, and enthalpy of mixing of liquid alloy over the wide range of composition and temperature.

JUNMO JEON, DANIEL LINDBERG, and MIN-KYU PAEK are with the Department of Chemical and Metallurgical Engineering, Aalto University, Espoo, 02150, Finland. Contact e-mail: min.paek@aalto.fi SUN-YONG KWON is with the Department of Mining and Materials Engineering, McGill University, Montreal, QC, H3A 0C5, Canada.

Manuscript submitted July 2, 2020 and accepted September 27, 2020.

Article published online October 27, 2020.

The liquid solution properties in Ni-based alloys and Co-based alloys were first compiled by Sigworth *et al.*^[10,11] using Wagner's formalism, respectively. They reported many thermodynamic data such as the standard Gibbs free energy of solution, activity coefficient of various alloying elements at the infinitely dilute solution, and interaction parameters between alloying elements and impurities in both the Ni and Co alloy melts. However, their interaction parameters can be used only for the dilute concentration range at a limited temperature under the C saturated condition. Moreover, their ternary interaction parameters for the effect of Co on C in Ni melt^[10] and that of Ni on C in Co melt^[11] cannot be merged to predict the thermodynamic behavior of C over the whole composition of Ni-Co melt because each parameter is only valid in the selected solvent, Ni or Co in this formalism.

For the framework of phase diagram construction, the Scientific Group Thermodata Europe (SGTE)^[12] and the European Cooperation in the Field of Scientific and Technical Research (COST 507)^[13] have developed the thermodynamic database based on the Bragg–Williams (BW) random mixing model. The previous optimizations in Ni-C and Co-C systems^[14–16] have reproduced the thermodynamic properties of solid phases and phase diagram information well over the entire range of composition and temperature, but considerable inconsistencies remain between the measured enthalpy of mixing data^[17,18] and the model predictions in the liquid solution. Witusiewicz *et al.* have measured the partial enthalpy of mixing of C in dilute Ni and Co solutions as 45.0^[17] and 93.7 kJ/mol,^[18] respectively, with respect to the graphite reference state at 1873 K (1600 °C). However, these values were back-calculated as 5.9^[15] and 19.2 kJ/mol^[16] by the previous optimizations. The previous modeling results from insufficient experimental data may not reasonably reproduce the enthalpy of mixing data. In addition, the conventional regular solution model based on the ideal random configuration of atoms generally cannot simultaneously explain the Gibbs free energy and the enthalpy of mixing data when the liquid solution has a very strong interaction or significant asymmetry.

The authors' recent studies showed that the strong interactions between liquid metal and gaseous impurities such as C,^[19,20] N,^[21] and O^[22,23] could be precisely described by taking into account the short-range ordering (SRO) using the modified quasichemical model (MQM) in the pair exchange reaction.^[24] Therefore, the MQM was adopted for the description of the strong attraction force of C and asymmetric liquid solution properties in the Ni-C, Co-C, and Ni-Co-C systems. To check the validity of the modeling result, the C solubility was measured in liquid Ni at 1673 K to 1873 K (1400 °C to 1600 °C) and Ni-Co alloys at 1673 K (1400 °C), respectively. The asymmetry of Ni-C and Co-C systems was reproduced by putting more weight on the reported partial enthalpy of mixing of the C data available in the literature,^[17,18] which have been scarcely considered by the previous CALPHAD (CALculation of PHase Diagram) modeling. Even though the Ni-Co binary liquid solution exhibits almost ideal behavior with a very

small positive enthalpy of mixing around 0.35 kJ/mol at maximum, it was reevaluated using the MQM for model consistency. By taking an asymmetric interpolation method for the Gibbs free energy of the liquid solution in the ternary Ni-Co-C system, the C solubility data in the liquid Ni-Co-C alloy were successfully reproduced without any additional ternary model parameters.

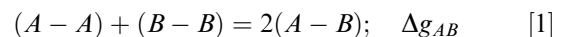
II. EXPERIMENTS AND ANALYSES

To verify the asymmetric property of the binary and ternary liquid solutions, the C solubility was measured over the wide range of melt composition from pure Ni to Ni-57.5 mass pct Co alloy by the equilibration and quenching method. The experiments were carried out in a MoSi₂ resistance furnace (Nabertherm RHTV 120-150/18) at 1673 K, 1773 K, and 1873 K (1400 °C, 1500 °C, and 1600 °C). The temperature of the hot zone in an alumina reaction tube with 30 mm inner diameter was measured by S-type Pt/Pt-10 mass pct Rh thermocouple. The desired portion of high-purity metallic Ni (99.996 pct purity) and sponge Co (99.99 pct purity) was charged in a graphite crucible [outer diameter (OD): 10 mm, inner diameter (ID): 6 mm, height (H): 20 mm] and then placed in the center of the hot zone at the predetermined reaction temperature under an Ar atmosphere. By the preliminary experiments, it was confirmed that the time required for the C dissolution from the graphite crucible was 2 hours at 1673 K (1400 °C). Therefore, the alloys were equilibrated for 2 hours in all sets of experiments. The samples were quenched by dropping the sample in ice water and cut for the chemical analyses. The sectioned samples were polished to remove the excess graphite formed during cooling and solidification. The C content was analyzed by the combustion method with a thermal conductive detector (Thermo Scientific, Thermo Flash Smart EA CHNS/O with MV). The Ni and Co contents were analyzed using inductively coupled plasma-optical emission spectroscopy (ICP-OES, Perkin Elmer Optima 7100DV).

III. THERMODYNAMIC MODEL FOR LIQUID SOLUTION

The liquid solution properties in the binary Ni-C and Co-C systems were then thermodynamically analyzed over the entire composition range using the MQM in the pair approximation by considering the SRO. The detailed description and associated notations of the MQM in the binary and ternary systems are available elsewhere.^[22,24] The Gibbs free energies of pure liquid Ni, Co, and hypothetical liquid C were taken from thermodynamic data compilation by SGTE.^[12] All calculations were performed with the FactSage thermochemistry software for the optimization of liquid solution using the MQM.

In the MQM, the pair exchange reaction in a binary A–B liquid solution can be expressed as:



where $(i-j)$ represents the first-nearest neighbor (FNN) pair and Δg_{AB} is the Gibbs free energy change for the formation of two moles of $(A-B)$ pairs, respectively. Based on the pair approximation, the following mass balances are considered to account the pair distribution:

$$Z_A n_A = 2n_{AA} + n_{AB} \quad [2]$$

$$Z_B n_B = 2n_{BB} + n_{AB} \quad [3]$$

where n_i , n_{ij} , Z_A , and Z_B are the number of moles of component i and $(i-j)$ pair and the coordination numbers of A and B , respectively.

The Gibbs free energy of the liquid solution is given by:

$$G = (n_A g_A^\circ + n_B g_B^\circ) - T\Delta S^{\text{config}} + (n_{AB}/2)\Delta g_{AB} \quad [4]$$

where g_A° and g_B° are the molar Gibbs free energies of pure liquid phases that can be directly taken from SGTE.^[12] ΔS^{config} is an approximate expression for the configurational entropy of mixing with considering the random distribution of the $(A-A)$, $(B-B)$, and $(A-B)$ pairs on the basis of the ideal entropy of mixing in the one-dimensional Ising approximation^[24]:

$$\begin{aligned} \Delta S^{\text{config}} = & -R(n_A \ln X_A + n_B \ln X_B) \\ & - R \left[n_{AA} \ln \left(\frac{X_{AA}}{Y_A^2} \right) + n_{BB} \ln \left(\frac{X_{BB}}{Y_B^2} \right) + n_{AB} \ln \left(\frac{X_{AB}}{2Y_A Y_B} \right) \right] \end{aligned} \quad [5]$$

where X_i and X_{ij} are the mole fraction of i and the pair fraction of $(i-j)$ pair, respectively. Y_i is the coordination equivalent fraction of i calculated from the pair fractions, $Y_i = X_{ii} + X_{ij}/2$.

The Δg_{AB} in Eq. [4] can be expressed in terms of the pair fractions:

$$\Delta g_{AB} = \Delta g_{AB}^\circ + \sum_{i \geq 1} g_{AB}^{i0} X_{AA}^i + \sum_{j \geq 1} g_{AB}^{0j} X_{BB}^j \quad [6]$$

where Δg_{AB}° , g_{AB}^{i0} , and g_{AB}^{0j} are the model parameters as functions of temperature in the $A-B$ binary liquid solution.

The equilibrium pair distribution is calculated under the condition of

$$\left(\frac{\partial G}{\partial n_{AB}} \right)_{n_A, n_B} = 0 \quad [7]$$

According to a given Δg_{AB} value during the optimization, a different n_{AB} can be evaluated as a solution of Eq. [7], and then n_{AA} and n_{BB} can be obtained by Eqs. [2] and [3] with the coordination number information. To reproduce all available liquid solution properties, the optimum Δg_{AB} values are repeatedly searched.

In this model, the asymmetry of the liquid solution can be represented as a non-equimolar composition of maximum SRO in each binary system by setting the ratio of the coordination numbers, Z_B/Z_A , from the following equations:

$$\frac{1}{Z_A} = \frac{1}{Z_{AA}^A} \left(\frac{2n_{AA}}{2n_{AA} + n_{AB}} \right) + \frac{1}{Z_{AB}^A} \left(\frac{n_{AB}}{2n_{AA} + n_{AB}} \right) \quad [8]$$

$$\frac{1}{Z_B} = \frac{1}{Z_{BB}^B} \left(\frac{2n_{BB}}{2n_{BB} + n_{AB}} \right) + \frac{1}{Z_{BA}^B} \left(\frac{n_{AB}}{2n_{BB} + n_{AB}} \right) \quad [9]$$

where Z_{AA}^A and Z_{AB}^A are the values of Z_A , when all nearest neighbors of an A are A and B s, respectively, and Z_{BB}^B and Z_{BA}^B are defined *vice versa*.

In the present study, the coordination numbers of pure elements, Z_{NiNi}^{Ni} , Z_{CoCo}^{Co} , and Z_{CC}^C , were set to 6. Since the Ni-Co binary liquid solution exhibits the ideal behavior, $Z_{NiCo}^{Ni}/Z_{NiCo}^{Co}$ was set to 1 ($= 6/6$). Thus, the Z_{Ni} and Z_{Co} are fixed as the constant value 6 over the whole composition range of binary Ni-Co liquid solution. On the other hand, Z_{NiC}^C/Z_{NiC}^{Ni} and Z_{CoC}^C/Z_{CoC}^{Co} were set to 4 ($= 8/2$) to describe the asymmetry of liquid solution with the maximum SRO near $X_C = 1/5$ in both the Ni-C and Co-C systems. All the values of the coordination numbers selected in the present study are listed in Table I.

After optimizing three sub-binary liquid parameters, the Gibbs free energy of the ternary Ni-Co-C liquid solution was estimated. Using the proper interpolation method depending on the intrinsic property of each constituent in the sub-binary systems, the absolute value or the number of ternary model parameters can be minimized. In case of an asymmetric ternary system, the Toop-like interpolation method can be beneficial to prevent a mathematical failure in the middle of the ternary triangle.^[25] Therefore, the non-metallic element, C, was set as the asymmetric component in the ternary Ni-Co-C system under the Toop-like interpolation method.

The Gibbs free energies of all solid phases have been accurately modeled using the compound energy formalism (CEF) in the Ni-C system by Lee^[15] and Co-C, Ni-Co, and Ni-Co-C systems by Guillermet.^[16,26,27] Therefore, these stable solid phases were retained to be compatible with the previous database because they have been widely used for the calculation of solid-phase equilibria in the various multicomponent systems.

IV. RESULTS AND DISCUSSION

A. The Ni-C Binary System

The Ni-C binary is a simple eutectic system as shown in Figure 1. The liquid Ni alloy is in equilibrium with graphite at high temperature, and the face centered cubic (FCC) solid solution has limited carbon solubility in the Ni-rich side at low temperature. There are no stable carbide phases in this system. Gabriel *et al.*^[14] thoroughly reviewed the available thermodynamic data of liquid and solid solutions, and they have assessed the Gibbs free energies of liquid and FCC solid solutions. For the description of liquid Gibbs energy, they used the regular solution model. However, the previous concept of the two-sublattice model was used by considering the

Table I. Optimized Liquid MQM Parameters for Ni-C, Co-C, Ni-Co, and Ni-Co-C Systems

Liquid (L)	MQM: (Ni,Co,C)
$Z_{NiNi}^{Ni} = Z_{CoCo}^{Co} = Z_{CC}^C = Z_{NiCo}^{Ni} = Z_{NiCo}^{Co} = 6$	
$Z_{NiC}^{Ni} = Z_{CoC}^{Co} = 2, Z_{NiC}^C = Z_{CoC}^C = 8$	
$g_{Ni(l)}, g_{Co(l)}, g_{C(l)}$	[12]
$\Delta g_{NiC}, J/mol$	$-24476 + 6.339T + (4812 - 4.293 T)X_{NiNi} + (1.979 T)X_{NiNi}^2$
$\Delta g_{CoC}, J/mol$	$-10000 - 4.393T - (1046)X_{CoCo} + (2.929 T)X_{CoCo}^2$
$\Delta g_{NiCo}, J/mol$	444
$g_{NiCo(C)}^{001}, J/mol$	0

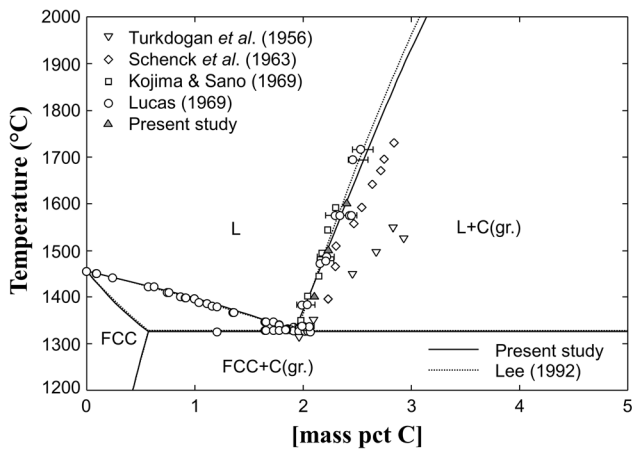


Fig. 1—Calculated phase diagram of the Ni-C system together with the experimental data.^[29–32]

transformation of C from Ni free graphite to hypothetical Ni carbide with the interaction between vacancy and C in the interstitial sublattice of the FCC solid solution. Later, Lee^[15] revised the Ni carbide end-member formation Gibbs energy in FCC without considering the nickel-free graphite based on the analytical expression by Hillert and Staffansson.^[28] Then, the interaction parameters of FCC and liquid solution were adjusted to improve the reproducibility of the C solubility in both FCC and liquid solutions as well as to keep the measured eutectic point. The previous assessments^[14,15] reasonably reproduced not only the C solubility but also the activity of C data in FCC measured at various temperatures by controlling the carburizing gas mixture, CH₄/H₂. The calculated C solubility in liquid Ni also corresponds well with the experimental results within the experimental error range. However, as mentioned earlier, the measured enthalpy of mixing data^[17] in the Ni-C liquid solution was not considered by the previous assessments.^[14,15]

The C solubility in the liquid Ni alloy shows large scatter as shown in Figure 1. This is attributed to the experimental difficulty and analytical limit of C. In general, a lower C content among the reported values has been preferred because it is not easy to completely avoid the crystallization of graphite by the decreasing C solubility during the cooling and solidification of the alloy. Therefore, to verify the accuracy of the C

solubility in liquid Ni among the different data sets, the solubility limit of C in liquid Ni was measured at 1673 K, 1773 K, and 1873 K (1400 °C, 1500 °C, and 1600 °C) by the rapid quenching technique. The present experimental data of the C solubility were plotted along with the previous experimental results as shown in Figure 1. The present data agreed very well with the C solubility measured by Lucas^[29] at the high temperature region within the experimental error range. He also carried out fast quenching experiments by dropping the sample in water after equilibration. Then, the excess graphite formed on the surface was removed before the C analysis. Although Kojima and Sano^[30] measured the C solubility using relatively inaccurate control of the reaction temperature by a pyrometer, their results agreed well with the data measured by Lucas^[29] and the present study. On the other hand, the experimental data by Schenck *et al.*^[31] and Turkdogan *et al.*^[32] showed a more significant temperature dependence on the C solubility in liquid Ni from the eutectic point. To reproduce these selected experimental data including the present study, the Δg_{NiC}^o value was determined first. The constant term of this value is also strongly related to the enthalpy of mixing in the liquid solution. Then, the first-order parameter of the (Ni-Ni) pair, g_{NiC}^{10} , was adjusted to fit the significantly inclined eutectic composition to the Ni-rich side. The sharply increased C solubility in liquid Ni can be reproduced only with the temperature-dependent term of the second-order parameter of the (Ni-Ni) pair, g_{NiC}^{20} .

Figure 2 shows the partial enthalpy of mixing in the Ni-C melt at 1873 K (1600 °C) measured by Witusiewicz *et al.*^[17] using high-temperature isothermal calorimetry. Their experimental data with respect to the graphite reference state were converted to the hypothetical liquid C using the enthalpy of fusion of C, 117369 J/mol, compiled in the SGTE database.^[12] Thus, the partial enthalpy of mixing curves were also calculated over the entire C concentration range under the suppression of graphite formation. At low C content up to $X_C = 0.05$, the partial enthalpy of C shows an almost constant value, but it suddenly increases above the inflection point. Compared to the partial enthalpy of mixing of C in liquid Fe shown as a dashed line,^[33] the enthalpy value in liquid Ni is more positive while it shows stronger asymmetry with the C content than liquid Fe. To reproduce such significant asymmetry of the Ni-C

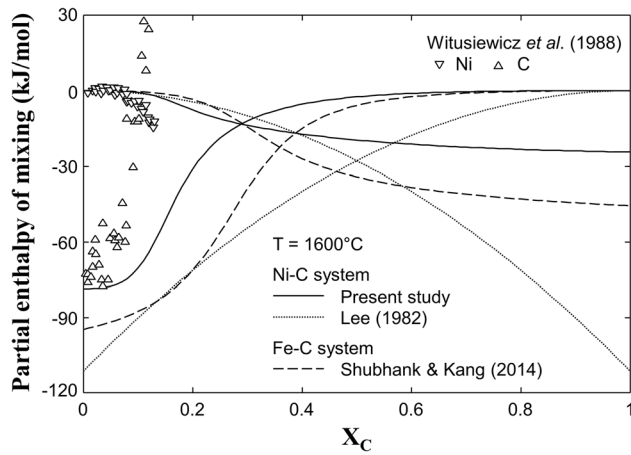


Fig. 2—Calculated partial enthalpy of mixing of Ni and C in liquid Ni-C alloy at 1873 K (1600 °C) by MQM (solid line) and the random mixing model (dotted line)^[15] along with the experimental data.^[17] The dashed line is the calculated partial enthalpy of mixing in the Fe-C system using MQM.^[33]

liquid solution, the ratio of the $Z_{\text{NiC}}^{\text{C}}/Z_{\text{NiC}}^{\text{Ni}}$ in the MQM was set to 4 ($= 8/2$), which is higher than $Z_{\text{FeC}}^{\text{C}}/Z_{\text{FeC}}^{\text{Fe}} = 2$ ($= 6/3$) in the Fe-C system.^[33] As shown in the figure, the partial enthalpy of mixing of C at higher X_{C} (> 0.05) was not well reproduced despite the consideration of SRO in liquid Ni alloy. As mentioned by Biletski *et al.*,^[34] this can be attributed to the fact that the delay of the complete dissolution of C at the high C concentration region causes a lack of heat generation during mixing. On the other hand, the partial enthalpy of C data measured at low C concentration had relatively higher accuracy because of the shorter dissolution time. Therefore, the enthalpy of mixing data at only the dilute C concentration was used for modeling the liquid solution. However, the random mixing model calculation is greatly underestimated even at the infinitely dilute concentration of C in liquid Ni shown as a dotted line in the figure.

Figures 3 and 4 show the calculated enthalpy and entropy of mixing in the liquid Ni-C alloy at 1873 K (1600 °C), respectively, with respect to pure liquid Ni and hypothetical liquid C. As shown in Figure 3, the present model can explain the asymmetric enthalpy of mixing data evaluated from the partial enthalpy data of Ni and C.^[17] However, the symmetric random mixing model needs more negative enthalpy terms to reproduce the asymmetric property of the liquid solution. This leads to a very negative entropy of mixing by putting much bigger positive temperature terms shown as the dotted line in Figure 4, whereas the present calculation with smaller temperature terms was less deviated from ideality. From the Gibbs energy function, $\Delta G = \Delta H - T\Delta S$, it is expected that a more stable liquid solution can be secured at higher temperatures by the positive entropy of mixing. Therefore, this approach can prevent the modeling failure at high temperatures such as the formation of inverted stable solid solution phases or the liquid miscibility gap.^[33]

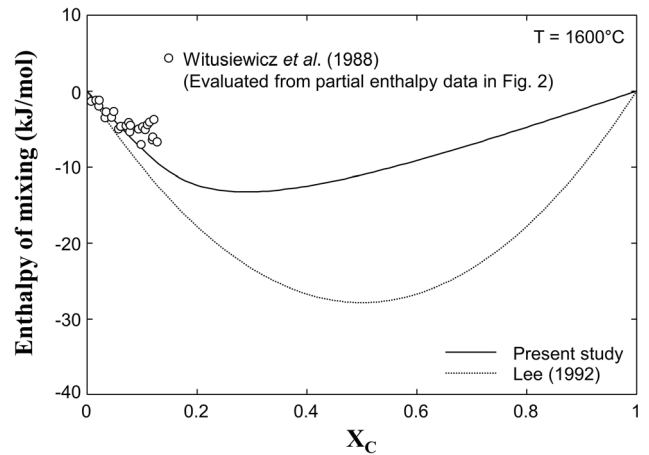


Fig. 3—Calculated integral enthalpy of mixing in liquid Ni-C alloy at 1873 K (1600 °C) along with the experimental data.^[17]

B. The Co-C Binary System

The Co-C binary also has a simple eutectic reaction by liquid solution \rightleftharpoons FCC + graphite as shown in Figure 5. No stable Co carbide has been observed below the eutectic temperature. As a standard state of Co, the hexagonal close-packed (HCP) structure becomes stable on the Co-rich side with negligibly small C solubility. Since the Gibbs energy description of FCC and HCP by Guillermet^[16] was directly used in this study, the low temperature region for the eutectoid reaction (FCC \rightleftharpoons HCP + graphite) was not shown in the figure. The liquid model parameter was reassessed by using the MQM to simultaneously reproduce the liquidus, solidus, and eutectic point^[35–37] as well as the C solubility data in liquid Co.^[30–32,38,39] Compared to the Ni-C system, the C content at the eutectic composition in the Co-C system is slightly higher around 0.5 mass pct. No verification experiment was required because the reported C solubility data in liquid Co were more consistent with each other than those of liquid Ni. Among the previous data, the experimental values of Patterson *et al.*^[36] and Schenck *et al.*^[31] were mainly used to fit the phase boundaries in the Co-C system. Based on the $\Delta g_{\text{CoC}}^{\circ}$ term, the asymmetric effect was adjusted by the first-order parameter of the (Co-Co) pair, g_{CoC}^{10} , without temperature dependence. Like the Ni-C system, only the temperature-dependent term was required for the second-order parameter of the (Co-Co) pair, g_{CoC}^{20} , to explain the increasing tendency of C solubility with temperature.

Figure 6 shows the partial enthalpy of mixing of Co and C in the binary liquid solution measured by Witusiewicz and Shumikhin^[18] using high-temperature isothermal calorimetry with respect to the liquid Co and C at 1873 K (1600 °C). As already mentioned in Section IV. A, their results of partial enthalpy of C were quite scattered and sharply increased with C content due to the delay of C dissolution during the heat content measurement. Thus, the liquid model parameters in the binary Co-C system were determined to best fit the enthalpy of mixing of C data at dilute C

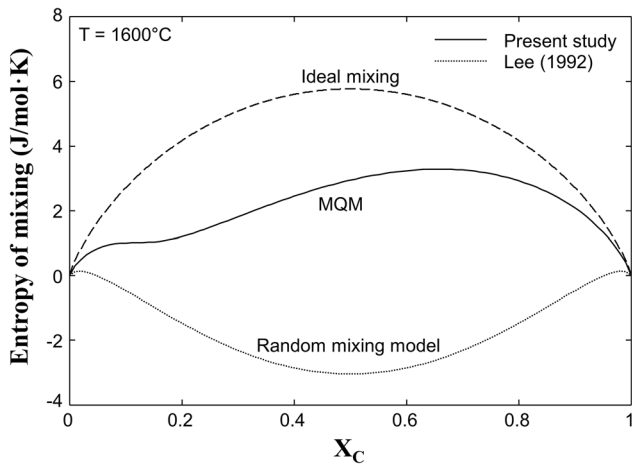


Fig. 4—Calculated entropy of mixing in liquid Ni-C alloy at 1873 K (1600 °C) by the MQM (solid line) and random mixing model (dotted line).^[15] Dashed line is the calculated ideal entropy of mixing.

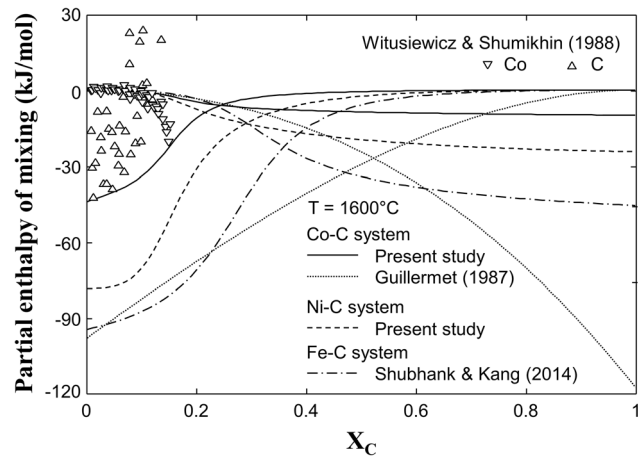


Fig. 6—Calculated partial enthalpy of mixing of Co and C in liquid Co-C alloy at 1873 K (1600 °C) by MQM (solid line) and the random mixing model (dotted line)^[15] along with the experimental data.^[18] Comparison of calculated partial enthalpy of mixing by MQM in the Ni-C system from the present study (dashed line) and in the Fe-C system from Shubhank and Kang.^[33]

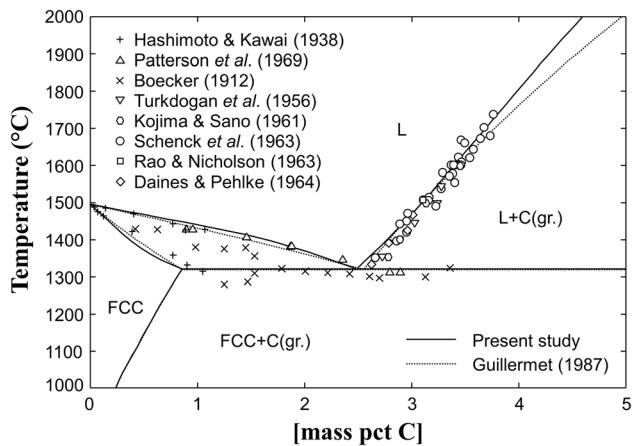


Fig. 5—Phase diagram of the Co-C system together with the previous experimental data.^[30–32,35–39]

concentration. The calculated partial enthalpy of mixing of C at the infinitely dilute solution of Co alloy was determined as -44.2 kJ/mol, which is a more positive value than that of Ni alloy (-78.7 kJ/mol) shown as the dashed line in this figure. The ratio of the $Z_{\text{CoC}}^{\text{C}}/Z_{\text{CoC}}^{\text{Co}}$ in the MQM was kept as 4 ($= 8/2$) to describe the asymmetric partial properties. It was also sufficient to have a similar eutectic composition between the Co-C system (2.5 mass pct C) and Ni-C system (1.9 mass pct C), which are much more inclined to the alloy-rich side than the Fe-C system (4.2 mass pct C). As Figure 5 shows, the optimization of the Co-C system by Guillermet^[16] has no problem with calculating the phase diagram. However, the enthalpy of mixing of C at dilute Co solution calculated by his parameters using the random mixing model was -98.1 kJ/mol, which is more than twice the measured value (dotted line in Figure 6). This means that the enthalpy of mixing by the previous

assessment was significantly underestimated, and the entropy contribution to the Gibbs free energy may be inaccurate.

Using the MQM, the excess entropy can be minimized because the model can internally consider the non-configurational effect by the pair formation and its distribution for the calculation of configurational entropy by Eq. [5]. As shown in Figure 7, the configurational entropy of the regular solution model is always fixed with composition under the random distribution of atoms in the liquid solution. On the other hand, the calculated configurational entropy in Co-C, Ni-C, and Fe-C liquid solutions using the MQM varies from the ideal entropy depending on the SRO. The configurational entropy in the Co-C and Ni-C systems at their eutectic point shows the maximum deviation from the ideal mixing at $X_{\text{C}} = 1/5$ because of the selected coordination number ratio, $Z_{\text{CoC}}^{\text{C}}/Z_{\text{CoC}}^{\text{Co}} = Z_{\text{NiC}}^{\text{Ni}}/Z_{\text{NiC}}^{\text{Ni}} = 4$. The Fe-C solution has the maximum deviation at its SRO composition, $X_{\text{C}} = 1/3$, by the higher value of coordination number ratio, $Z_{\text{FeC}}^{\text{C}}/Z_{\text{FeC}}^{\text{Fe}} = 2$.

Figure 8 shows the variation of the coordination numbers, Z_{Ni} , Z_{Co} , Z_{Fe} , and Z_{C} calculated by Eqs. [8] and [9] according to the C concentration in the Ni-C, Co-C, and Fe-C liquid solution, respectively. The calculated Z_{C} value in the Fe-C liquid solution is fixed as six by setting $Z_{\text{FeC}}^{\text{C}} = Z_{\text{CC}}^{\text{C}} = 6$. Except for Z_{C} , the coordination numbers changed with the C content. It can be noted that the maximum SRO composition corresponded well with the inflection points of the Z_{Ni} , Z_{Co} , and Z_{Fe} curves. This result emphasized that the degree of SRO can affect the configuration of atoms in the liquid solution. By considering such a non-configurational effect for the configurational entropy calculation, the temperature-dependent terms in the excess Gibbs free energy can be reduced. Given the modeling

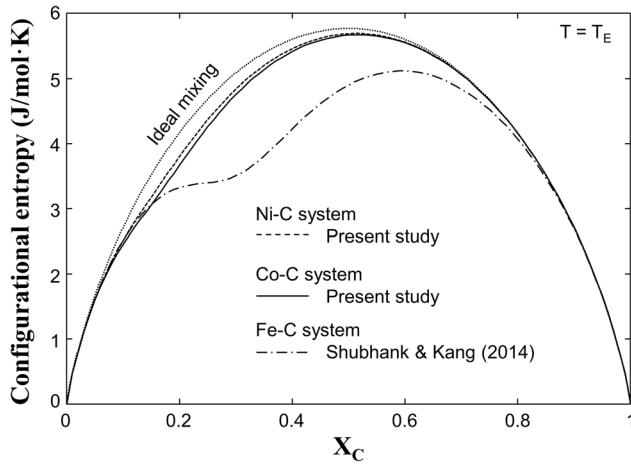


Fig. 7—Configurational entropy of mixing in ideal (dotted line), Ni-C (dashed line), Co-C (solid line), and Fe-C (dash-dot line) liquid solution at eutectic temperature, T_E .

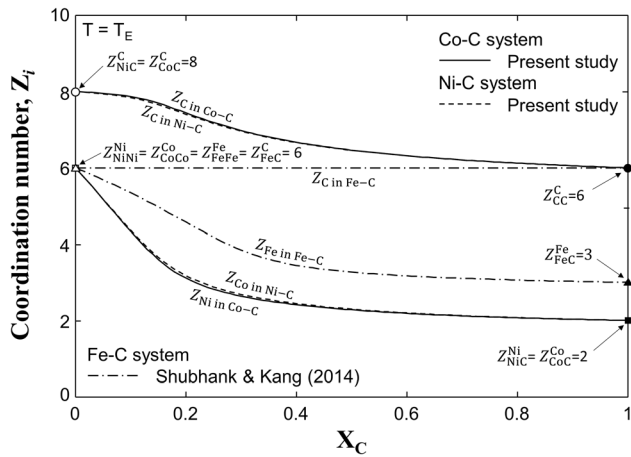


Fig. 8—Variation of the coordination number with X_C in Ni-C (dashed line), Co-C (solid line), and Fe-C (dash-dot line) liquid solution at eutectic temperature, T_E .

procedure, it is also beneficial to minimize the high-order parameters for expanding the system to the multicomponent system.

C. The Ni-Co-C Ternary System

The ternary Ni-Co-C system has been optimized by Guillermet^[27] using the random mixing model for the liquid solution and the CEF for the solid phases, respectively. They extensively reviewed all available thermodynamic data in this system. According to their evaluations, there are four phases such as liquid solution, FCC, HCP solid solutions, and graphite. As mentioned earlier, the present study only adopted the Gibbs free energy description of solid phases from the previous assessments^[15,16,27] and reassessed the liquid solution by the MQM. Prior to the ternary liquid optimization, the binary Ni-Co liquid solution was checked. Even though the Ni-Co liquid solution is considered an ideal solution because of the very small

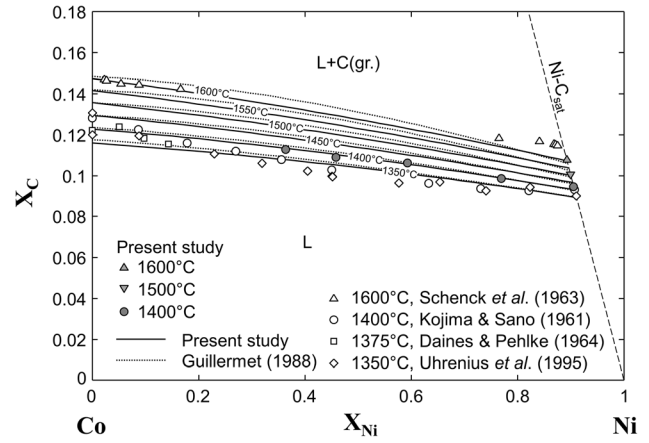


Fig. 9—Calculated C solubility in Ni-Co-C liquid alloy at 1623 K to 1873 K (1350 °C to 1600 °C) along with the present and previous experimental data.^[30,31,38,40]

positive deviation of both activity and enthalpy of mixing data from the ideality,^[26] the binary MQM parameter was determined as a constant value for consistency with other sub-binaries. By combining all binary MQM parameters determined in the present study, the liquid solution properties in this ternary system were explained without the ternary model parameter. The Toop-like asymmetric approximation^[25] with C as the asymmetric component was used because the liquid Ni-C and Co-C solutions exhibit considerable negative deviation by the SRO, while the liquid Ni-Co system shows almost ideal behavior.

Figure 9 compares the calculated C solubility in the Ni-Co alloy melt along with the available experimental results at 1623 K to 1873 K (1350 °C to 1600 °C).^[30,31,38,40] From the Co-rich side, the C solubility decreased with increasing Ni concentration in the Ni-Co alloy melt. Kojima and Sano^[30] and Uhrenius *et al.*^[40] have measured the C solubility over the entire alloying concentration range at 1673 K and 1623 K (1400 °C and 1350 °C), respectively. Kojima and Sano measured the C solubility using a high-frequency induction furnace.^[30] The alloy melt was rapidly equilibrated under a CO atmosphere for 2 hours and sampled by the quartz tube suction. However, the melt temperature was measured by an optical pyrometer. Uhrenius *et al.*^[40] used a horizontal resistance furnace, and the temperature was measured at the hot zone by a thermocouple. They mixed the metallic powder to get the target composition and charged it in a graphite crucible for 24 hours. However, their raw materials such as Co and Ni powder contained many impurities. Daines and Pehlke^[38] measured the C solubility in the Co-rich alloy melt up to 15.6 mass pct Ni at 1648 K (1375 °C) using the resistance furnace with intermittent manual stirring. However, the C content was evaluated by weighing the samples before and after the equilibration. Even though the previous experiments have their own error sources as mentioned above, the overall tendency of the C solubility data in the Ni-Co-C alloy melt reasonably agreed with the present calculation except for the data at the Ni-rich corner measured by Schenk *et al.*^[31] They

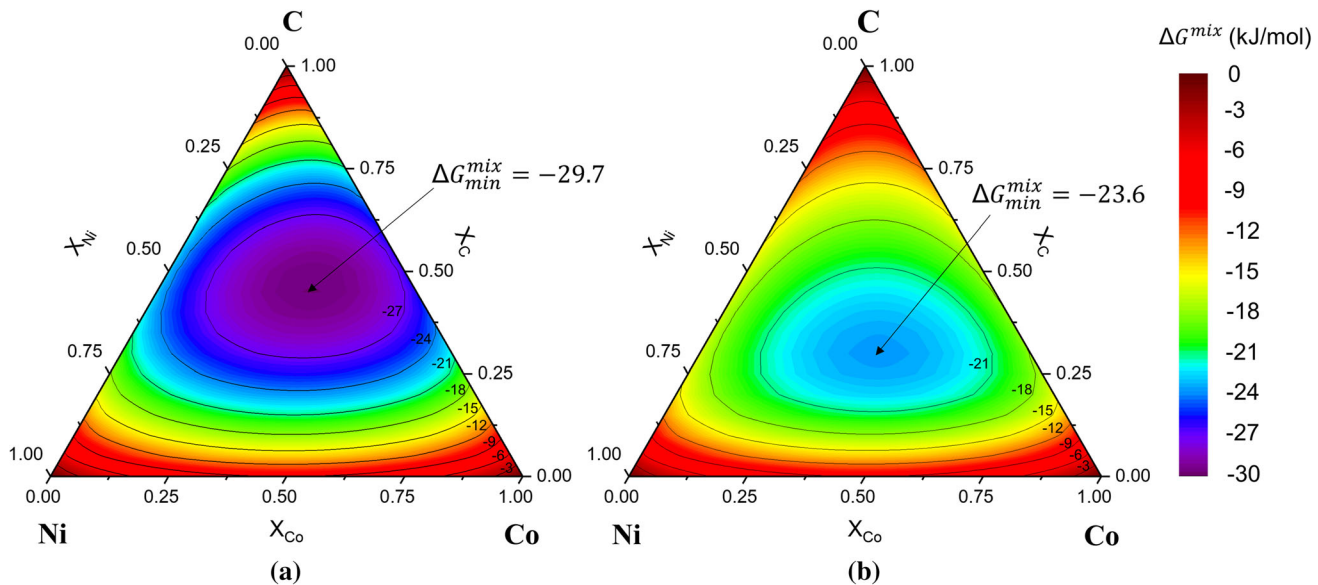


Fig. 10—Gibbs energy surface calculated by the (a) symmetric^[27] and (b) asymmetric interpolation method at 1623 K (1350 °C).

reported only a change of C solubility (ΔX_C) in the ternary system based on their C solubility data of the Ni-C binary melt. As mentioned in Section IV-A, their C solubility in liquid Ni was much higher than in the other set of experimental data; thus, the C solubility in the ternary melt may be overestimated. The deviation between the present model calculation and the reported data at the low temperature region was also verified by measuring the C solubility in Ni-Co-C melts over the wide Co concentration region from pure Ni to Ni-57.5 mass pct Co melts at 1673 K (1400 °C). The present experimental results are in good agreement with the predicted solubility curve as shown in Figure 9. The C solubility data measured by Kojima and Sano^[30] and Uhrenius *et al.*^[40] change parabolically with a minimum value near $X_{Ni} = 0.5$. It should be noted that the minimum C solubility can be obtained when the liquid solution is more stable at a certain composition. However, it is not easy to have a significantly negative interaction near the equimolar composition on the basis of the positive interaction between Ni and Co in the Ni-Co binary solution.

Although the previous model calculation showed similar results of the C solubility in liquid Ni-Co-C alloy with the present calculation, very large ternary parameters were added for both the constant and temperature-dependent term, $L_{C,Co,Ni}^{liq} = 50,462 - 27.562T$.^[27] This can be caused by describing the asymmetric liquid solution properties using the symmetric thermodynamic model with the Muggianu interpolation technique.^[41] Figure 10 shows the Gibbs energy surface calculated near the eutectic temperature of the Ni-Co-C system by the symmetric Muggianu method (Figure 10(a))^[27] and asymmetric Toop-like interpolation method (Figure 10(b)). The symmetric method forms the minimum Gibbs free energy of mixing near the center of the ternary triangle as shown in Figure 10(a). To reproduce the C solubility data at the

Ni-Co-rich side in this ternary system, the Gibbs free energy of liquid solution was adjusted on the whole by adding a large ternary model parameter. On the other hand, the present calculation using the asymmetric method forms the minimum Gibbs energy near $X_C = 0.3$ without any additional ternary parameter, as shown in Figure 10(b).

Figure 11 shows the predicted iso-activities of Ni, Co, and C (Figure 11(a)) and the iso-enthalpy of mixing (Figure 11(b)) in Ni-Co-C liquid solution at 1773 K (1500 °C) using the present database. Even though the measured activity data were only available in the Ni-rich corner^[42] or Co-rich corner,^[43] it is believable that the accuracy of iso-activity curves in the middle of this diagram has been secured because of the ideality of the Ni-Co binary liquid solution as well as no additional ternary parameter in the Ni-Co-C system. Figure 11(b) shows the predicted enthalpy of mixing over the entire composition from the Ni-Co side to the C saturated condition in the Ni-Co-C liquid solution. The enthalpy information can be used to precisely control the temperature during the battery scrap recycling process as well as the refining process of the superalloys.

V. CONCLUSION

In the Ni-Co-C ternary system, the liquid solution has been reassessed using the MQM to analyze all available thermodynamic properties related to the Gibbs free energy and enthalpy of mixing simultaneously. This proves that the individual contribution of the enthalpy and entropy to the Gibbs energy of the liquid solution is better represented by considering SRO. The predictability of partial enthalpy of mixing of C in both Ni-C and Co-C systems was much improved compared to the random mixing model. By introducing the asymmetric interpolation technique, no additional ternary

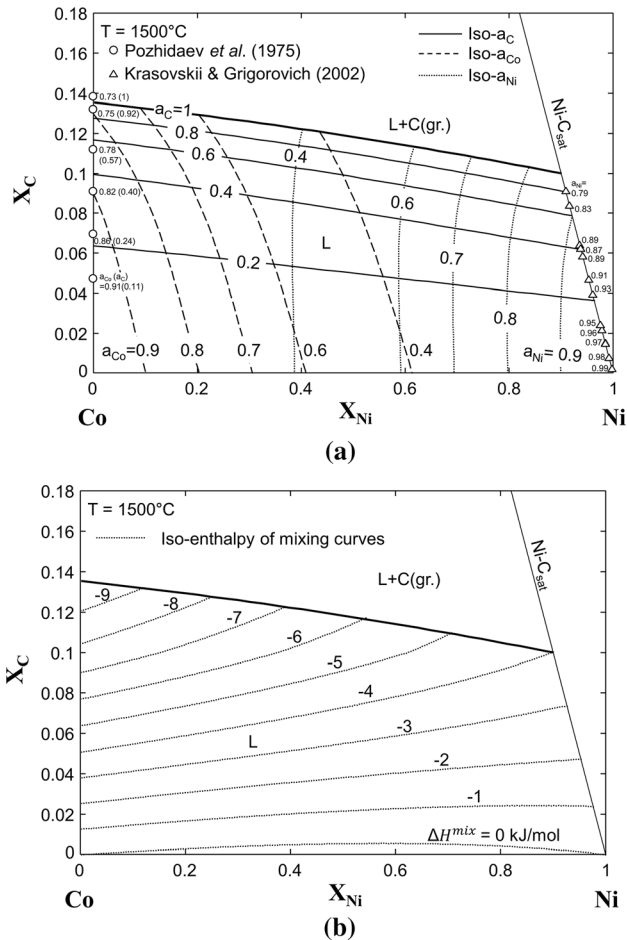


Fig. 11—(a) Calculated iso-activity and (b) iso-enthalpy of mixing curves in Ni-Co-C liquid solution at 1773 K (1500 °C).

parameter was required to reproduce the C solubility and activity in the ternary Ni-Co-C liquid solution. This database will be further developed by adding other alloying elements and impurities such as Cu, Fe, O, and S. Therefore, it can be used to predict the distribution ratio of Ni and Co among slag, matte, and alloy as well as the heat transfer during the Ni slag cleaning stage of the Ni flash smelting process and the refining of superalloys.

ACKNOWLEDGMENTS

Funding from the Steel and Metals Producers Foundation (Teknologiategollisuuden 100-Vuotisjuhlasäätiö) and Business Finland, SYMMET project (Grant Number 3891/31/2018) is greatly appreciated. This study utilized the Academy of Finland's RawMatTERS Finland Infrastructure (RAMI), based jointly at Aalto University, GTK, and VTT.

This article is licensed under a Creative Commons Attribution 4.0 International License, which permits use, sharing, adaptation, distribution and reproduction in any medium or format, as long as you give appropriate credit to the original author(s) and the source, provide a link to the Creative Commons licence, and indicate if changes were made. The images or other third party material in this article are included in the article's Creative Commons licence, unless indicated otherwise in a credit line to the material. If material is not included in the article's Creative Commons licence and your intended use is not permitted by statutory regulation or exceeds the permitted use, you will need to obtain permission directly from the copyright holder. To view a copy of this licence, visit <http://creativecommons.org/licenses/by/4.0/>.

FUNDING

Open access funding provided by Aalto University.

REFERENCES

1. D. Wang, W. Liu, X. Zhang, Y. Huang, M. Xu, and W. Xiao: *Int. J. Photoenergy*, 2019, vol. 2019, pp. 1–13.
2. X.P. Gao, S.M. Yao, T.Y. Yan, and Z. Zhou: *Energy Environ. Sci.*, 2009, vol. 2, pp. 502–05.
3. H.S. Klapper, N.S. Zadorozne, and R.B. Rebak: *Acta Metall. Sin.*, 2017, vol. 30, pp. 296–305.
4. H. Huan, A. Mandelis, L. Liu, and A. Melnikov: *NDT&E Int.*, 2017, vol. 87, pp. 44–49.
5. W.Z. Wang, T. Jin, J.H. Jia, J.L. Liu, and Z.Q. Hu: *Mater. Sci. Eng. A*, 2015, vol. 624, pp. 220–28.
6. S. van den Brink, R. Kleijn, B. Sprecher, and A. Tukker: *Resour. Conserv. Recycl.*, 2020, vol. 156, p. 104743.
7. G.X. Ren, S.W. Xiao, M.Q. Xie, B. Pan, J. Chen, F.G. Wang, and X. Xia: *Trans. Nonferrous Met. Soc. China*, 2017, vol. 27, pp. 450–56.
8. T. Müller and B. Friedrich: *J. Power Sources*, 2006, vol. 158, pp. 1498–1509.
9. T. Georgi-Maschler, B. Friedrich, R. Weyhe, H. Heegn, and M. Rutz: *J. Power Sources*, 2012, vol. 207, pp. 173–82.
10. G.K. Sigworth, J.F. Elliott, G. Vaughn, and G.H. Geiger: *Metall. Soc. CIM*, 1977, vol. 16, pp. 104–10.
11. G.K. Sigworth and J.F. Elliott: *Can. Metall. Q.*, 1976, vol. 15, pp. 123–27.
12. A.T. Dinsdale: *CALPHAD*, 1991, vol. 15, pp. 317–25.
13. J.E. Tibballs: *COST 507 – Thermochemical databases for light alloys*, European Communities, Luxembourg, 1988, vol. 2.
14. A. Gabriel, C. Chatillon, and I. Ansara: *High Temp. Sci.*, 1988, vol. 25, pp. 17–54.
15. B.J. Lee: *CALPHAD*, 1992, vol. 16, pp. 121–49.
16. A.F. Guillermet: *Z. Metallkde.*, 1987, vol. 78, pp. 700–709.
17. V.T. Witusiewicz, A.K. Biletski, and V.S. Shumikhin: *Metally*, 1988, vol. 4, pp. 61–64.
18. V.T. Witusiewicz and V.S. Shumikhin: *Rasplavy*, 1988, vol. 2, pp. 72–75.
19. M.K. Paek, J.J. Pak, and Y.B. Kang: *CALPHAD*, 2014, vol. 46, pp. 92–102.
20. A.T. Phan, M.K. Paek, and Y.B. Kang: *Acta Mater.*, 2014, vol. 79, pp. 1–15.

21. M.K. Paek, S. Chatterjee, J.J. Pak, and I.H. Jung: *Metall. Mater. Trans. B*, 2016, vol. 47B, pp. 1243–62.
22. M.K. Paek, J.J. Pak, and Y.B. Kang: *Metall. Mater. Trans. B*, 2015, vol. 46B, pp. 2224–33.
23. M.K. Paek, K.H. Do, Y.B. Kang, I.H. Jung, and J.J. Pak: *Metall. Mater. Trans. B*, 2016, vol. 47B, pp. 2837–47.
24. A.D. Pelton, S.A. Degterov, G. Eriksson, C. Robelin, and Y. Dessureault: *Metall. Mater. Trans. B*, 2000, vol. 31B, pp. 651–59.
25. A.D. Pelton: *CALPHAD*, 2001, vol. 25, pp. 319–28.
26. A.F. Guillermet: *Z. Metallkde.*, 1987, vol. 78, pp. 639–47.
27. A.F. Guillermet: *Z. Metallkde.*, 1988, vol. 79, pp. 524–36.
28. M. Hillert and L.I. Staffansson: *Acta Chem. Scand.*, 1970, vol. 24, pp. 3618–26.
29. L.D. Lucas: *Mém. Sci. Rev. Métall.*, 1969, vol. 10, pp. 747–55.
30. Y. Kojima and K. Sano: *Tetsu-to-Hagané*, 1961, vol. 47, pp. 897–902.
31. H. Schenck, M.G. Froberg, and E. Steinmetz: *Arch. Eisenhüttenwes.*, 1963, vol. 34, pp. 37–42.
32. E.T. Turkdogan, R.A. Hancock, and S.I. Herlitz: *J. Iron Steel Inst.*, 1956, vol. 182, pp. 274–77.
33. K. Shubhank and Y.B. Kang: *CALPHAD*, 2014, vol. 45, pp. 127–37.
34. A.K. Biletski, V.T. Witusiewicz, and V.S. Shumikin: *Metally*, 1984, vol. 6, pp. 40–45.
35. U. Hashimoto and N. Kawai: *J. Jpn. Inst. Met.*, 1938, vol. 2, pp. 26–28.
36. W. Patterson, S. Engler, and R. Moser: *Giessereiforschung*, 1969, vol. 21, pp. 51–63.
37. G. Boecker: *Metallurgie*, 1912, vol. 9, pp. 296–303.
38. W. Daines and R.D. Pehlke: *Trans. ASM*, 1964, vol. 57, pp. 1011–15.
39. K.K. Rao and M.E. Nicholson: *Trans. AIME*, 1963, vol. 227, pp. 1029–30.
40. B. Uhrenius, K. Forsén, B.O. Haglund, and I. Andersson: *J. Phase Equilib.*, 1995, vol. 16, pp. 430–40.
41. Y.M. Muggianu, M. Gambino, and J.P. Bros: *J. Chim. Phys.*, 1975, vol. 72, pp. 83–88.
42. R.V. Krasovskii and K. Grigorovich: *Russian Metall.*, 2002, vol. 2002, pp. 21–29.
43. Y.V. Pozhidaev, B.P. Burylev, J.E. Dobrovinsky, and V.D. Ivanova: *Izv. Vys. Ucheb. Zaved. Chernaya Metallurgiya*, 1975, vol. 12, pp. 11–13.

Publisher's Note Springer Nature remains neutral with regard to jurisdictional claims in published maps and institutional affiliations.